

Projectile-charge dependence of inner-shell-ionization cross sections in a high-velocity region

K. Ishii, K. Sera, and A. Yamadera

Cyclotron and Radioisotope Center, Tohoku University, 980 Sendai, Japan

M. Sebata, H. Arai, and S. Morita*

Department of Physics, Faculty of Science, Tohoku University, 980 Sendai, Japan

(Received 1 July 1981)

Ratios of ionization cross sections for proton impact to those for ^3He -ion impact have been measured on AK and YL shells at projectile energies of 7, 9, 12, 16, and 21 MeV/amu. The ratio tends to unity with an increase in the projectile energy for both the AK and YL ionizations. This behavior can well be explained in terms of the Binstock-Reading theory combined with the distant-collision theory of Hill and Merzbacher: The polarization effect in distant collisions and the decreasing electron-density effect in close collisions cancel out each other in this high-energy region.

I. INTRODUCTION

Inner-shell ionizations by heavy-charged particles have been calculated in terms of the plane-wave Born approximation (PWBA),¹ binary-encounter approximation (BEA),² and semiclassical approximation (SCA).³ An extensive series of experimental studies have been carried out in the region of $V_p \lesssim V_e$, where V_p is the projectile velocity and V_e is the velocity of an orbital electron to be ionized, and detailed comparisons with theoretical predictions have been reported. In accordance with these simple theories, the inner-shell-ionization cross section is in proportion to the square of the projectile charge Z_i : The ratio between the ionization cross section divided by Z_i^2 for two kinds of projectiles of the same velocity

$$R \equiv Z_2^2 \sigma(Z_1) / Z_1^2 \sigma(Z_2) \quad \text{with } Z_1 > Z_2$$

should be unity. From the experimental point of view, the ratio of ionization cross sections measured under the same experimental condition can be obtained with a high accuracy because of cancellation of large errors coming from the target thickness, corrections for absorption in window material and air path, and from the detection efficiency including the solid angle for the detector. Hence, the experimental result of the ratio provides a rigorous test of theoretical predictions.

The result on R obtained heretofore shows regular deviations from unity^{4,5}: In a region of very

low projectile velocity, R is considerably larger than unity and this deviation has been explained by the Coulomb deflection effect. With an increase in the projectile velocity, R decreases and becomes less than unity. This behavior has been well interpreted in terms of the effect of increase in the binding energy. After reaching a minimum, R begins to increase since collisions of large impact parameter become effective with an increase in the projectile energy and the two effects mentioned above disappear; R becomes again larger than unity because of the polarization effect, which implies an effect of increase in the electron density near the projectile due to the attractive force of the projectile. In the region near $V_p \simeq V_e$, the electron transfer from the target atom to the projectile plays an important role and it gives rise to the maximum in the ratio; afterward the ratio decreases again with an increase in the projectile velocity.

In the region of $V_p \gg V_e$ experimental studies on inner-shell ionization are still scarce; in particular, no measurement of the projectile-charge dependence has been done. On the other hand, theoretical calculations of the ratio have been carried out by Basbas *et al.*,⁵ and by Binstock and Reading.⁶ Basbas *et al.*⁵ have estimated the contribution of the polarization effect in the high-energy region in terms of the distant-collision theory and have shown that this effect makes the ratio R larger than unity. On the other hand, Binstock and

Reading⁶ have evaluated the effect in terms of the Glauber approximation and obtained the result that the ratio R in the high-energy region is less than unity, in contrast to the prediction by Basbas *et al.* Binstock and Reading have interpreted this fact as follows: The polarization effect makes an increase in the electron density in the vicinity of the projectile—increasing-density effect—while it makes a decrease in a distant region—decreasing-density effect—and in the high-energy region the decreasing-density effect becomes predominant more than the increasing-density effect. Hence, R becomes less than unity with an increase in the projectile energy. Their result is not consistent with the result of Basbas *et al.* This discrepancy results from the fact that the effect of polarization of the atom *as a whole* is estimated from the distant-collision theory, while the Glauber approximation gives a *local* change in the electron density, which is expected to affect the ionization by close collisions. It is therefore desirable to develop a theory on the basis of the ionization mechanism discussed in our previous paper.⁷

The aim of the present work is to obtain the ratio R in the region $V_p \geq V_e$ with high accuracy by measuring the AlK and YL x-ray production cross sections for proton and 3He bombardments and to compare the results with the theoretical predictions of the effects mentioned above. The polarization effect in the high-energy region is also discussed on the basis of ionization mechanism.⁷

II. EXPERIMENTAL PROCEDURE AND RESULTS

Targets of $100\text{-}\mu\text{g}/\text{cm}^2$ thick Al and $40\text{-}\mu\text{g}/\text{cm}^2$ thick Y were bombarded with beams of protons and doubly ionized 3He ions with energies of 7, 9, 12, 16, and 21 MeV/amu, accelerated with the Tohoku University AVF cyclotron. The whole experimental setup has been reported elsewhere.⁷ The beam energy has been determined to an accuracy of 0.1% with a beam-analyzing magnet, which is set in a beam-transport line other than that shown in Fig. 1 of Ref. 7. The beam was focused to a 3-mm-diam spot on the target. The Al target was self-supporting and the Y target was prepared by vacuum-evaporating Y onto a Mylar foil of $4\text{-}\mu\text{m}$ thickness. AlK and YL x rays have been measured with an ORTEC Si(Li) detector of energy resolution of 160 eV for 6.4-keV x rays through a Ta slit of 3-mm diameter. The detector

was set at 135° with respect to the beam. When the charge state of a projectile changes in passing through a target, the number of projectiles cannot be evaluated simply from the beam current, and the x-ray yield may not be proportional to the beam current. Such an effect has actually been observed in experiments of heavy-ion impact.⁸ By using the semiempirical formula for average equilibrium charge,⁹ however, it is estimated that the charge state of protons and $^3He^{2+}$ ions changes within a range of 0.1% in the present energy region. Thus the target-thickness effect on the charge state and the change of charge state due to the $4\text{-}\mu\text{m}$ Mylar backing can be neglected in the present work. The ionization energies of AlK and YL shells are, respectively, 1.56 and 2.37 keV, so that the projectile velocity V_p at 21 MeV/amu is a factor of 2.7 larger than the velocity V_e of AlK electrons. Electric pulses from the detector were analyzed with a minicomputer (MELCOM 35/70) and have been stored in magnetic tapes. The mean beam current had been kept at several nanoamperes and the counting rates has been about 100 counts/sec in order to prevent a pileup effect.

At each bombarding energy, measurements on Al and Y targets were alternately repeated twice in order to check a fluctuation of the measuring condition. Since the measurements for protons and 3He ions were carried out under the same experimental conditions, errors in the target thickness, the detection efficiency, the solid angle, the fluorescence yield, and the correction for absorptions cancel out in the ratio of the cross sections for protons to those for 3He ions: the ratio is directly given by

$$R = Y_{^3He} / 4Y_p ,$$

where $Y_{^3He}$ and Y_p are the counts per projectile, respectively, for 3He -ion and proton impact. In the case of YL x rays, anisotropic angular distribution induced by the inner-shell alignment¹⁰ must be taken into consideration. However, the deviation from the isotropy for the present bombarding energy is estimated to be smaller than 0.1% and can be neglected.

Energy losses of proton and 3He -ion beams in the Al and Y targets were estimated and it was found that differences in the effective energy between the proton and 3He -ion beams are only 0.2 and 0.5%, respectively, for the Al and Y targets at 7 MeV/amu, and 0.03 and 0.01%, respectively, for the Al and Y targets at 20 MeV/amu. Errors of

the cross sections coming from the energy loss can therefore be neglected. Therefore, the error of R originates from the statistical fluctuation of the counts, the background subtraction, uncertainty of integrated beam currents, nonuniformity of the targets, and the difference in energies for protons and ^3He ions. Among these, the statistical fluctuation is negligible owing to the large counts.

Typical spectra obtained for the Al and Y targets at 21 MeV/amu are shown in Figs. 1(a) and 1(b). Assuming a Gaussian shape for the characteristic x-ray peak and a polynomial of the sixth order for the background, the spectra were fitted with the least-squares method as shown with solid curves in the figures. These backgrounds consist of the secondary-electron bremsstrahlung,¹¹ the quasifree-electron bremsstrahlung,¹² and γ rays and neutrons from nuclear reactions; the low-energy continuum x rays are much reduced by absorption in the beryllium window of the Si(Li) detector, the air path, and the 10- μm Mylar window of the target chamber. In Fig. 1(a), the depression of the background in the middle of the peak can be understood as the result of overlapping of the decreasing-continuum x rays with the neutron background which becomes predominant in the lowest energy region. In the case of Y L x rays shown in Fig. 1(b), the continuum x rays play an

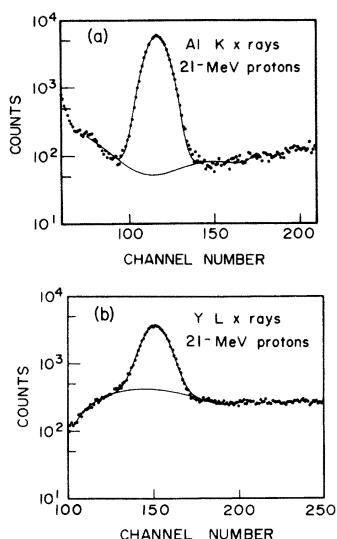


FIG. 1. (a) and (b) Typical spectra of Al K—(a)—and Y L—(b)—x rays obtained from 21-MeV proton bombardments. The solid curves were calculated by fitting to the experimental results with the least-squares method, assuming a Gaussian shape for the characteristic x-ray peak and a polynomial of the sixth order for the background.

important role in the background. Thus the backgrounds fitted with the least-squares method seem to be quite reasonable within the ambiguity determined from the statistical errors. The error due to the background subtraction ϵ_B is therefore estimated from

$$\epsilon_B = \frac{\sum_i \sqrt{n_B(i)}}{\sum_i n(i)},$$

where $n_B(i)$ are the background counts in a channel i obtained from the least-squares method, $n(i)$ are the signal counts, and the summation is taken over the channel range which gives 90% of the total signal counts. Values of ϵ_B thus estimated are smaller than 0.1% in the present experiment.

The data obtained on the Al and Y targets, alternately repeated twice, are shown in Table I. Fluctuations of the data are considered to be due to the error of integrated beam currents and the nonuniformity of the targets, and the data are consistent within 0.5% for Al and 1% for Y. The

TABLE I. Uncertainty of the data for Al K- and Y L-shell ionizations.

E_p	Target	Counts/n Coulomb		
		(1)	(2)	(1)/(2)
6.893	Al	12.416	12.437	0.998
6.893	Y	8.0609	8.0747	0.998
9.003	Al	11.057	11.154	0.991
9.003	Y	7.5418	7.6987	0.980
12.07	Al	9.5813	9.5766	1.000
12.07	Y	6.8888	6.8578	1.005
16.02	Al	7.8686	7.8376	1.004
16.02	Y	5.9827	5.9554	1.005
20.80	Al	6.7860	6.7373	1.007
20.80	Y	5.0831	5.0985	0.997
$E_{^3\text{He}}$	Target	Counts/n Coulomb		
		(1)	(2)	(1)/(2)
$E_{^3\text{He}}$				
20.78	Al	52.492	52.320	1.003
20.78	Y	34.048	34.066	0.999
27.04	Al	46.448	46.302	1.003
27.04	Y	31.976	31.890	1.003
35.57	Al	39.104	39.404	0.992
35.57	Y	28.896	28.402	1.017
47.50	Al	32.034	32.212	0.994
47.50	Y	24.170	24.524	0.986
63.98	Al	26.656	26.726	0.997
63.98	Y	20.254	20.030	1.011

larger value for Y might be due to the Y target evaporated on a Mylar film.

In order to obtain the value of R , the cross section for proton impact must be compared with that for ^3He -ion impact with the same velocity. To do this the yields, divided by the projectile number and square of the projectile charge and multiplied by the projectile energy, are plotted as a function of the energy in logarithmic scale and are shown for AlK and YL x rays in Figs. 2(a) and 2(b), respectively, where almost straight lines are obtained. In this figure, the yield for ^3He ions with the same velocity as protons was estimated from interpolation of the ^3He line corresponding to a given value of proton energy. Since energies of the proton and ^3He -ion beams have been measured to

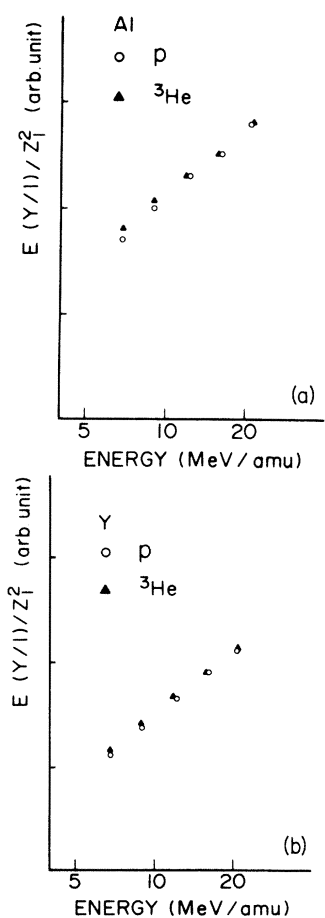


FIG. 2. (a) and (b) The x-ray yields, divided by the projectile number and square of the projectile charge and multiplied by the projectile energy, are plotted as a function of the logarithm of the projectile energy (MeV/amu) for AlK- and YL-shell ionizations in (a) and (b), respectively.

TABLE II. Experimental ratios R of the AlK shell and the YL shell.

E (MeV/amu)	Al	Y
6.890	1.054	1.055
8.966	1.042	1.047
11.79	1.012	1.026
15.75	1.010	1.010
21.21	0.998	1.001

an accuracy of 0.1% and the measurements have been carried out at nearly equal beam energies for these two beams, the errors corrected for by this process are quite small and are not larger than the experimental errors of the data. The results of R thus obtained are shown in Table II. Uncertainties of these values are estimated to be 1 and 2% for Al and Y, respectively. Figure 3 represents the results for AlK-shell ionization together with the results obtained by Basbas *et al.*⁵ Both results are quite consistent with each other. Figure 4 shows the present results for YL-shell ionization. As seen in these figures, R converges to unity with an increase in the projectile energy.

III. COMPARISONS WITH THEORIES AND DISCUSSION

A. The Glauber approximation

Reading and Fitchard,¹³ Binstock and Reading,⁶ and Golden and McGuire¹⁴ have applied the Glauber approximation to the calculation of the K-shell ionization cross section for light-ion impact. On the basis of the Glauber theory, Reading

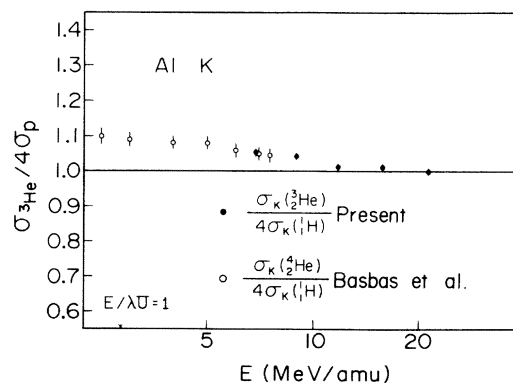


FIG. 3. The present experimental results of the ratio R for AlK-shell ionizations are shown together with those obtained by Basbas *et al.*⁵

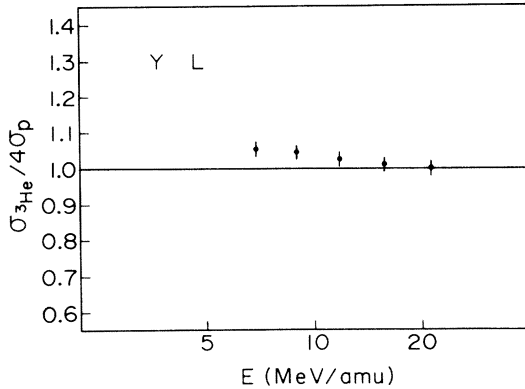


FIG. 4. The present experimental results of the ratio R for Y - L -shell ionizations.

and Fitchard have derived formulas for the AlK -shell ionization in terms of the Glauber approximation and the Cheshire approximation, which will be described below, and the results are compared with the experimental results in Fig. 5, respectively, by the dotted line and the solid line. Binstock and Reading⁶ have developed a more accurate approximation, as will be described below, and the results are shown by the dot and dashed curve in Fig. 5. It is seen in this figure that the ratio R approaches unity with an improvement of the approximation: the contribution of decreasing-density effect becomes smaller. The best approximation of R by Binstock and Reading shows a crossover behavior at $E = 7.8$ MeV/amu and predicts a value of R about 5% less than unity in the energy region of $E \geq 12$ MeV/amu, in contrast to the present experimental result.

B. The perturbed-stationary-state approximation

Basbas *et al.* have calculated the effect of the orbital-electron polarization on the inner-shell ionization cross section by using the theory of Hill and Merzbacher¹⁵ on the basis of the perturbed-stationary-state approximation. On the other hand, Morgan and Sung¹⁶ have estimated a contribution of the polarization effect to the stopping power in terms of the second-order Born approximation. The results of calculation by Basbas *et al.* are compared with the experiment in Fig. 6, where the solid curve was obtained by taking account of the effect of the orbital-electron polarization and the dotted curve was obtained by adding the effect of electron capture by the projectile to the solid curve. In the intermediate-energy region, the calculation

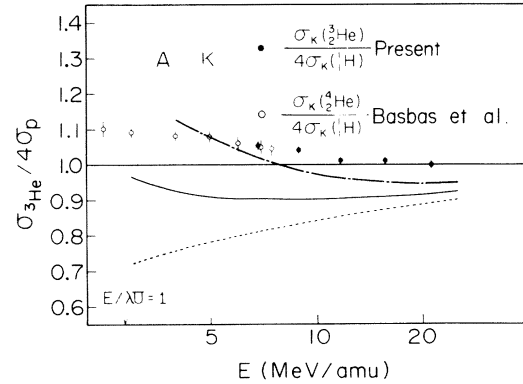


FIG. 5. The experimental results on AlK -shell ionizations are compared with the theoretical predictions from the Glauber approximation; the dotted, the solid, and the dot and dashed curves show the results of calculations by Glauber, Cheshire, and Binstock and Reading, respectively.

produces rather well the experimental result, whereas in the high-projectile-velocity region, the agreement is not so good. It can also be seen in Fig. 6 that the electron transfer is little effective in the present energy region.

C. The Glauber approximation combined with the distant-collision theory of Hill and Merzbacher

In conformity with the Glauber approximation, a scattered initial wave function is expressed by

$$\psi_i = e^{i \vec{k} \cdot \vec{R}} \psi_{1s}(\vec{r}) S(\vec{R}, \vec{r}), \quad (1)$$

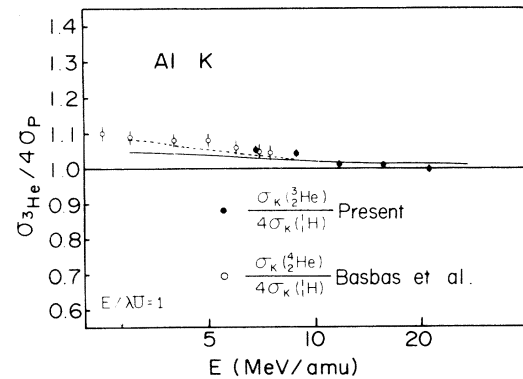


FIG. 6. Comparison of the experimental results with the calculations based on the perturbed-stationary-state approximation. The solid curve calculated by Basbas *et al.* shows the effect of the orbital-electron polarization and the dotted curve further takes account of the effect of electron capture by the projectile.

where $\psi_{1s}(\vec{r})$ is the wave function of the 1s-state electron and K is the wave number of the projectile. The function $S(\vec{R}, \vec{r})$ is to be derived from

$$i\hbar v \frac{\partial}{\partial z} S(\vec{R}, \vec{r}) = \left[\tilde{H}_e - \frac{z_1 e^2}{|\vec{R} - \vec{r}|} \right] S(\vec{R}, \vec{r}), \quad (2)$$

with

$$\begin{aligned} \tilde{H}_e &= -\frac{\hbar^2 \nabla_r^2}{2m_e} + \frac{\hbar^2}{m_e a_s} \frac{\partial}{\partial r} \\ &\equiv \tilde{\mathcal{F}} + \tilde{\mathcal{B}} \end{aligned}$$

and

$$a_s = \frac{a_0}{Z},$$

where \vec{R} and \vec{r} are the position vectors for, respectively, the projectile and the electron with respect to the target atomic nucleus, a_0 is the Bohr radius, z_s is the effective nuclear charge, m_e is the electron rest mass, v is the projectile velocity, and $\tilde{\mathcal{F}}$ and $\tilde{\mathcal{B}}$ are called, respectively, the freely recoiling term and the binding term.

The approximation of $\tilde{H}_e = 0$ in Eq. (2) is called the Glauber approximation. The Cheshire approximation of setting $\tilde{\mathcal{B}} = 0$ leads $S(\vec{R}, \vec{r})$ to be the Coulomb wave function in the projectile field: the orbital electron is scattered by the projectile as a free electron. Hence, this approximation refers to the Rutherford scattering between the projectile and the atomic electron—a close collision.¹⁷ Binstock and Reading have calculated $S(\vec{R}, \vec{r})$ by taking account of both $\tilde{\mathcal{F}}$ and $\tilde{\mathcal{B}}$ terms but neglecting the exchange term between them.

In the present case of $V \gg V_0$, where V_0 is the average velocity of the orbital electron, a solution of Eq. (2) is approximately given by¹⁸

$$S(\vec{R}, \vec{r}) = e^{-i\tilde{H}_e z/\hbar v} \exp \left[\frac{i}{\hbar v} \int_{-\infty}^z V_I dz' \right] \quad (3)$$

with

$$V_I = e^{i\tilde{H}_e z/\hbar v} \frac{-z_1 e^2}{|\vec{R} - \vec{r}|} e^{-i\tilde{H}_e z/\hbar v}.$$

The operator $e^{i\tilde{H}_e z/\hbar v}$ in Eq. (3) is modified by

$$\begin{aligned} e^{i\tilde{H}_e z/\hbar v} &= e^{(iz/\hbar v)\tilde{\mathcal{F}}} e^{(iz/\hbar v)\tilde{\mathcal{B}}} \exp \left[-\frac{1}{2} \left[\frac{iz}{\hbar v} \tilde{\mathcal{F}}, \frac{iz}{\hbar v} \tilde{\mathcal{B}} \right] \right] \\ &= e^{(iz/\hbar v)\tilde{\mathcal{F}}} e^{(iz/\hbar v)\tilde{\mathcal{B}}} e^{(iz/\hbar v)g(r)\tilde{\mathcal{F}}'}. \end{aligned} \quad (4)$$

Here,

$$g(r) = i \frac{v_0}{v} \frac{z}{r}, \quad (5)$$

$$\tilde{\mathcal{F}}' = \tilde{\mathcal{F}} + \frac{\hbar^2}{2m_e} \left[\frac{\partial^2}{\partial r^2} + \frac{1}{r} \frac{\partial}{\partial r} \right]. \quad (6)$$

If we assume that

$$\frac{z}{r} < 1, \quad (7)$$

the exchange term can be neglected. The effective value of z is estimated from the uncertainty principle by

$$z \approx 1/q,$$

where q is the transfer momentum of the projectile. Therefore, Eq. (7) becomes $qr > 1$, which means a close collision. The Binstock and Reading approximation should therefore be applicable to a close collision.

On the basis of the ionization mechanism and the PWBA theory, we^{7,17} recently divided the ionization cross sections into those for close and distant collisions, where a distant collision means a collision with an atom as a whole or a photoelectric ionization by virtual photons induced by the projectile: $qr < 1$. Consequently, if the Binstock and Reading calculation takes into account only close collisions, the contribution of the polarization effect to the ionization cross section is expressed by

$$\delta\sigma_C(z_1) = \frac{8\pi a_0^2}{z_s^4} \frac{z_1^2}{\eta_K} \int_{W_{\min}}^{\infty} \frac{dW}{W} \int_{Q_{\min}}^{\infty} \frac{dQ}{Q} F_K^{CC}(W, Q) \int_0^1 dx' F(c(1-x'^2)^{1/2}), \quad (8)$$

where η_K , W_{\min} , and Q_{\min} should be referred to by Merzbacher and Lewis.¹ The function $F_K^{CC}(W, Q)$ is the generalized oscillator strength of the K shell for close collisions and has been defined in the pre-

vious paper.⁷ The term $F(c(1-x'^2)^{1/2})$ represents the effect of the local change in the electron density and has been defined in Ref. 6. Values of R calculated from Eq. (8) are shown in Fig. 7, where

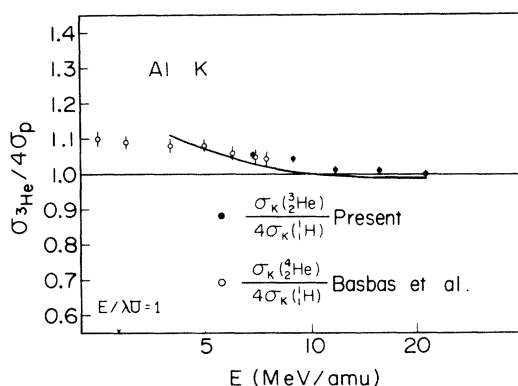


FIG. 7. Comparison between the experimental results and the calculation using the Glauber approximation in which the difference between close and distant collisions is taken into account.

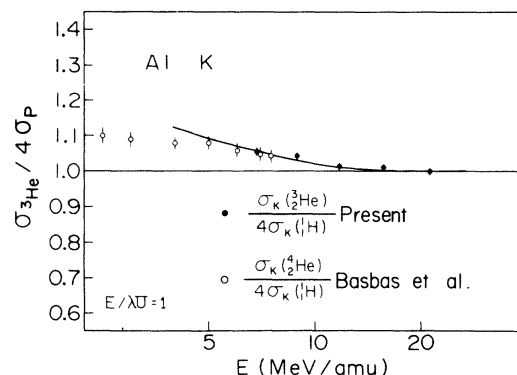


FIG. 8. Comparison between the experimental results and the calculation using the Glauber approximation combined with the perturbed-stationary-state theory [see Eq. (10) in the text].

it is seen that the decreasing-density effect is smaller than that estimated by Binstock and Reading (see Fig. 5).

As was mentioned above, the Glauber approximation is not applicable to the calculation of the polarization effect in distant collisions, whereas the distant-collision theory of Hill and Merzbacher or the second-order Born approximation is applicable. Using the theory of Hill and Merzbacher, Basbas *et al.*⁵ have estimated the contribution of the polarization effect in distant collisions, which were defined as the collisions of large parameter, and the result is given by

$$\delta\sigma_D(z_1) = \frac{6\pi^2 a_0^2}{z_s^5} \frac{z_1^3}{(\eta_k)^{5/2}} \left[\ln \left(\frac{4\eta_K}{\theta_K} \right) - 1.6 \right], \quad (9)$$

where θ_K is the screening constant defined by Merzbacher and Lewis.¹

Using the second-order Born approximation and the dipole approximation of $qr \ll 1$, Morgan and Sung¹⁶ have given the result nearly the same as Eq. (9).

As the result, the inner-shell ionization cross section for high-energy impact can be expressed by

$$\sigma^i(z_1) = \sigma_{\text{PWBA}}(z_1) + \delta\sigma_D(z_1) + \delta\sigma_C(z_1), \quad (10)$$

where σ_{PWBA} is the ionization cross section given

by Merzbacher and Lewis.¹ The predictions from Eq. (10) are compared with the experiments in Fig. 8, where the agreement is quite satisfactory. It is thus found that the polarization effect in distant collisions and the decreasing-density effect in close collisions cancel out each other in the high-energy region.

IV. CONCLUSION

The AlK and YL x-rays produced by bombarding the targets with protons and ^3He ion of 7–21 MeV/amu have been measured with a Si(Li) detector. The projectile-charge dependence of the ionization cross section was obtained with high accuracy. The ratio of the cross sections between the proton and ^3He -ion impact tends to unity in contrast to the Binstock and Reading prediction. However, by taking only close collisions into account, the discrepancy between the theory and the experiment seems to be removed.

ACKNOWLEDGMENTS

The authors would like to thank A. Ohmura, H. Ono, S. Kan, and Y. Saeki for operating the cyclotron throughout the experiment.

- *Present address: Research Center of Ion Beam Technology, Hosei University, Kajinocho 3-7-2, Koganei, 184 Tokyo.
- ¹E. Merzbacher and H. W. Lewis, in *Encyclopedia of Physics*, edited by S. Flügge (Springer, Berlin, 1958), Vol. 34, p. 166.
- ²J. D. Garcia, Phys. Rev. A 1, 280 (1970).
- ³J. M. Hansteen and O. P. Mosebekk, Nucl. Phys. A201, 541 (1973).
- ⁴G. Basbas, W. Brandt, and R. Laubert, Phys. Rev. A 7, 983 (1973).
- ⁵G. Basbas, W. Brandt, and R. Laubert, Phys. Rev. A 17, 1655 (1978).
- ⁶J. Binstock and J. F. Reading, Phys. Rev. A 11, 1205 (1975).
- ⁷K. Sera, K. Ishii, M. Kamiya, A. Kuwako, and S. Morita, Phys. Rev. A 21, 1412 (1980).
- ⁸R. K. Gardner, T. J. Gray, P. Richard, C. Schmiedekamp, K. A. Jamison, and J. M. Hall, Phys. Rev. A 15, 2202 (1977).
- ⁹P. Richard, *Method of Experimental Physics* (Academic, New York, 1980), Vol. 17, p. 130.
- ¹⁰M. Kamiya, Y. Kinefuchi, H. Endo, A. Kuwako, K. Ishii, and S. Morita, Phys. Rev. A 20, 1820 (1979).
- ¹¹K. Ishii, S. Morita, and H. Tawara, Phys. Rev. A 13, 131 (1976).
- ¹²A. Yamadera, K. Ishii, K. Sera, and S. Morita, Phys. Rev. A 23, 24 (1981).
- ¹³J. F. Reading and E. Fitchard, Phys. Rev. A 10, 168 (1974).
- ¹⁴J. E. Golden and J. H. McGuire, Phys. Rev. A 15, 499 (1977).
- ¹⁵K. W. Hill and E. Merzbacher, Phys. Rev. A 9, 156 (1974).
- ¹⁶S. H. Morgan, Jr. and C. C. Sung, Phys. Rev. A 20, 818 (1979).
- ¹⁷K. Sera, K. Ishii, A. Yamadera, A. Kuwako, M. Kamiya, M. Sebata, and S. Morita, Phys. Rev. A 22, 2536 (1980).
- ¹⁸J. F. Reading, Phys. Rev. A 6, 1642 (1970).